USING AIRBORNE LIDAR TO PREDICT LEAF AREA INDEX

Ali Farid, Ferdowsi University of Mashhad
Mohammad Bannayan, Ferdowsi University of Mashhad
Amin Alizadeh, Ferdowsi University of Mashhad
Soroosh Sorooshian, University of California, Irvine
Faculty of Agriculture, P.O. Box 91775-1163, Mashhad, Iran
Department of Civil and Environmental Engineering
University of California, Irvine, CA
afaridh@yahoo.com

ABSTRACT

Estimation of riparian forest structural attributes, such as the Leaf Area Index (LAI), is an important step in identifying the amount of water use in riparian forest areas. In this research, small-footprint lidar data were used to estimate biophysical properties of young, mature, and old cottonwood trees in the Upper San Pedro River Basin, Arizona, USA. Four metrics (tree height, height of median energy, ground return ratio, and canopy return ratio) were derived by synthetically constructing a large footprint lidar waveform from small-footprint lidar data which were compared to ground-based high-resolution Intelligent Laser Ranging and Imaging System (ILRIS) scanner images. These four metrics were incorporated into a stepwise regression procedure to predict field-derived LAI for different age classes of cottonwoods. This study applied the Penman-Monteith model to estimate transpiration of the cottonwoods using lidar-derived canopy metrics. These transpiration estimates compared very well to ground-based sap flux transpiration estimates indicating lidar-derived LAI can be used to improve riparian cottonwood water use estimates.

Key words: Lidar, Leaf Area Index, Riparian, San Pedro River Basin.

INTRODUCTION

Vegetation patterns and associated canopy structure influence landscape functions such as water use, biomass production, and energy cycles. The properties of vegetation and canopy must be quantified in order to understand their roles in landscapes and before management plans can be developed for the purpose of conserving natural resources. In arid and semi-arid regions, with high potential evaporative demand, the presence of perennial flow and verdant riparian corridors can constitute a major source of water use (net loss) in overall basin water budgets (U.S. Dept. of Interior, 2006). However, basin level riparian water use is difficult to estimate with standard micro-meteorological techniques due to the often narrow, non-uniform corridors, which violate the necessary fetch requirements of many of these systems (Goodrich et al., 2000). The narrow, non-uniform nature of typical riparian corridors also makes rapid measurement of critical canopy parameters for riparian evapotranspiration estimates, such as LAI, difficult and time consuming. Remote sensing offers approaches to overcome some of these limitations and uncertainties. In particular, multi-return airborne lidar can provide the capability to identify riparian tree species (Farid et al., 2006a) and age and canopy characteristics (Farid et al., 2006b).

Recent progress in three-dimensional forest characterization at the stand level mainly includes digital stereophotogrammetry, synthetic aperture radar, and lidar (light detecting and ranging). Lidar is a technique in which light at high frequencies, typically in the infrared wavelengths, is used to measure the range between a sensor and a target, based on the round trip travel time between source and target. Airborne Laser Scanning (ALS) is a measurement system in which pulses of light (most commonly produced by a laser) are emitted from an instrument mounted in an aircraft and directed to the ground in a scanning pattern. This method of recording the travel time of the returning pulse is referred to as pulse ranging (Wehr and Lohr, 1999). The type of information collected from this returning pulse distinguishes two broad categories of lidar sensors: discrete-return (small footprint) lidar devices and full-waveform (large footprint) recording devices. For forested environments, the result is a waveform indicative of the forest structure (i.e., from the top of the canopy, through the crown volume and understory layer, and finally to the ground surface). Previous studies model full-waveform characteristics for simple, unvegetated terrain (Gardner, 1992), and for one-dimensional surfaces (Abshire et al., 1994). Additionally, Blair and Hofton

(1999) demonstrated that vertical distribution of the discrete-return data is closely related to the full-waveforms recorded by waveform-recording devices when certain conditions are met, the most important being a high density of samples collected using a very small footprint (on the order of 25 cm).

The foundations of lidar forest measurements lie with photogrammetric techniques developed to assess tree height, canopy density, forest volume, and biomass. Airborne laser measurements were used in place of photogrammetric measurements to estimate forest heights and canopy density (Nelson et al., 1984) and forest volume or biomass (Maclean and Krabill, 1986; Nelson et al., 1988a; 1988b). For instance, Nelson et al. (1988b) predicted the volume and biomass of southern pine (Pinus taeda, P. elliotti, P. echinata, and P. palustris) forests using several estimates of canopy height and cover from small-footprint lidar, explaining between 53% and 65% of the variance in field measurements of these variables.

The primary objective of this research was to use a small-footprint lidar to derive various height metrics (maximum laser height, mean laser height, and canopy height) and model full-waveform characteristics in cottonwood trees in the San Pedro Riparian National Conservation Area (SPRNCA) in southeastern Arizona, USA. The SPRNCA is a globally important migratory bird route. Its cottonwood riparian forest supports a great diversity of species and is widely recognized as a regionally and globally important ecosystem (World Rivers Review, 1997). Additionally, lidar studies published at this point have shown success in several forest types with large-footprint lidar, but applications of small-footprint lidar have not progressed as far (Means, 2000), being limited mainly to measuring even-aged coniferous stands. Thus, the performance of lidar in cottonwood riparian forests remains untested and any related analytical and processing issues are yet to be identified.

The secondary objective of this study was to estimate LAI from various laser height metrics and synthetic large footprint lidar waveform for different age classes of cottonwood trees. Additionally, this study applied the Penman-Monteith model (Monteith and Unsworth, 1990) to estimate cottonwood transpiration using lidar-derived LAI, compared with transpiration measured by sap flow. Riparian cottonwood trees use water in proportion to their age and canopy shape (Schaeffer et al., 2000), and are especially large users of water in flood plains along rivers in semi-arid environments. More accurate quantification of riparian water use is required to manage basin water resources to maintain the economic, social, and ecological viability of these areas and ensure water for a growing human population in the basin. Cottonwoods of different age cannot be distinguished by multi-spectral methods. Because older cottonwoods exhibit a canopy that is more crowned in shape than the younger trees, differences in tree shape as a function of tree age led us to investigate the use of lidar to identify cottonwoods of different age classes and estimate LAI, both of which impact a tree’s water use.

STUDY AREA

The three study sites are located on the floodplain of the San Pedro River within the SPRNCA in southeastern Arizona, USA. The Escalante study site (31º 51´N, 110º 13´W; 1110m elevation) is about 1.2 km long north to south and 1.4 km wide east to west and is relatively flat. The Escalante study site is located along an intermittent reach of the river where the groundwater depth ranged from 4.3 to 4.5 m. This study site was used to estimate LAI from various laser height metrics and synthetic large footprint lidar waveform for different age classes of cottonwood trees. This study area is populated by young-to-old dense cottonwood stands with patches of cottonwood riparian forest located along the stream channel.

The Boquillas study site (31º 69´N, 110º 18´W; 1180m elevation) is located along an intermittent reach of the river where the groundwater depth ranged from 3.1 to 3.9 m. In contrast, the Lewis Springs study site (31º 33´N, 110º 07´W; 1250m elevation) is located along a perennially flowing reach of the San Pedro River where the groundwater depth ranged from 1.1 to 1.8 m. These two additional sites were used to apply the Penman-Monteith model to estimate cottonwood transpiration using lidar-derived LAI, compared with transpiration measured by sap flow for individual cottonwood trees within an isolated cluster of cottonwoods. The cottonwood trees at both sites were very similar in age and size characteristics.

DATA ACQUISITION

Ground Inventory Data

Ground validation data were collected from April 2003 to October 2004. Three different ages of cottonwood trees were included in the field sampling – young cottonwoods (less than 15 years), mature cottonwoods (16 to 50 years), and old cottonwoods (greater than 50 years). Stem diameters at breast height (dbh) (diameter measured at 1.37 m above the ground) were measured with a diameter tape and recorded to the nearest mm to discriminate between young, mature, and old cottonwood patches, based on river-specific equations that relate dbh to tree age (Stromberg, 1998).

A total of 41 cottonwood trees were used to determine LAI. Of the 41 cottonwoods, 9 old, 15 mature, and 17 young isolated trees were selected that were at least 6 m apart. A differential global positioning system (DGPS) was used to determine the location of each individual tree within sub-meter planimetric accuracy (5700 GPS, Trimble Navigation, Ltd., Sunnyvale, CA). We measured 4 points around each tree at the edge of the tree canopy. In addition, all tree locations were determined using 60-second static measurements with a 12-channel GPS receiver. The GPS antenna height varied between 1.8 m and 3.6 m, with an average height of 2.5 m. All measurements were collected during the leaf-off season. The lack of canopy foliage and the raised antenna in the old cottonwood stands reduced the error effects of forest canopies on GPS measurements. These trees were identified in the lidar dataset by matching field DGPS locations with the georeferenced lidar data.

The LAI was measured using a plant canopy analyzer (LAI 2000, Li-Cor, Inc., Lincoln, NE) in June 2003 for different age classes of cottonwoods. LAI readings were taken from the four cardinal directions around the base of each cottonwood tree by one sensor with a 90º view cap. The sensor was aligned along the canopy of the tree, as well as across the canopy. Measurements were made after sunset at dusk, when the sky is still illuminated, but after the direct beam radiation leaves the canopy.

In 2006, Gazal et al. measured sap flow of four cottonwood trees within an isolated cluster at each of the two study sites (Boquillas and Lewis Springs), using constant heat flow Granier-type probes (TDP-30 and TDP-80, Dynamax, Inc., Houston, TX).

Additionally, air temperature, relative humidity, solar radiation, wind speed and air pressure were measured at nearby meteorological towers located 3 km from the Boquillas intermittent stream site and 0.3 km from the Lewis Springs perennial stream site (Scott et al., 2000). For both perennial and intermittent stream sites, the measurements were recorded every 15 and 30 min, respectively. Stand transpiration was estimated for the period 1-11 June 2003 (DOY: 152-162), which corresponded to the timing of the lidar survey.

Lidar Datasets

The Optech ALTM 1233 (Optech, Inc., Toronto, Canada) was used to survey the study site on June 6, 2003. Characteristics of the ALTM 1233 include a scanning frequency of 28 Hz, a scan angle of ± 20º, a collection mode of first and last returns, and intensity of returns from a 1064 nm laser. The ALTM 1233 was mounted on a University of Florida plane flying at 750 m above the ground at a velocity of 60 m/s. The aircraft and ALTM 1233 configuration resulted in a cross track point spacing of 0.9 m, a forward point spacing of 2.1 m, and a footprint size of approximately 15 cm in diameter. The average ground swath width was 546 m and the entire study area was covered by 4 parallel flight lines. For the entire research area, 50% overlapping flight lines were used to ensure complete coverage, which generated approximately 2 million laser returns. The lidar data were processed and classified using the Optech REALM 3.0.3d software. Three data layers were produced from the classification: (1) ground last-return, (2) vegetation last-return and (3) vegetation first-return. The ground last return data layer was a robust representation of the terrain. For this study, vegetation last and vegetation first data layers were merged into a single vegetation class. The attributes of any given laser return not only include x, y, and z coordinate data but also an intensity return value (Farid et al., 2006a).

Ground Based Laser Scanner

The ground based laser scanner acquired for the study site on June 2004, was the Intelligent Laser Ranging and Imaging System-Three-Dimensional (ILRIS-3D, Optech, Inc., Toronto, Canada), with a vertical accuracy of 0.3 cm. The laser scanner fires a focused laser at ground targets and measures the target position based on laser travel time to the target and back to the sensor. The hit size is 1.5 cm in diameter at 50 meters from the scanner, which was the approximate distance. The laser scanner collects x, y, and z relative coordinates for every 1.5 cm hit scanned for a complete three dimensional image of the object. Distance between hits (resolution) was on average 0.2 cm. The resolution changes with distance between the target and the scanner.

Capturing an entire cottonwood tree canopy required two scans on opposite sides the tree. If three sub-meter accuracy GPS points can be located within each scanned image, the images can easily be merged. We placed three large cardboard boxes in the foreground of each cottonwood tree that was to be scanned and then secured a piece of rebar into the ground at the corner of each box. Fig. 1 shows the boxes in the foreground of one old cottonwood tree as an example (two scans on opposite sides the tree). These points on the ground were then georeferenced with a differential global positioning system (DGPS) at a later date. The corners of the boxes where the rebar was located allowed us to locate the georeferenced points in the scanned image. Then the x, y, and z coordinates of the images were given UTM values and sea level altitude values in meters. Unfortunately, due to our remote location which is covered by dense vegetation and the stream channel bank, only one scanned tree had georeferenced points with enough accuracy for the images to be merged accurately into a full canopy. The other trees had to be manually merged. Manually merging is a tedious process and only works if at least three common points can be located in each image that is to be merged. This limitation reduced the number of trees with fully scanned canopies to five. Therefore, of the 24 old and mature cottonwoods, 3 old and 2 mature cottonwood trees were selected.

Figure 1. Cardboard boxes in the (a) foreground and (b) back part of one of the old cottonwood trees (two scans on opposite sides the tree).

ANALYSIS

Modeling a Return Waveform and Comparing with Ground Based Laser Scanner

Our model for a large-footprint lidar waveform is constructed under the assumption that the shape of any waveform represents the vertical distribution of intercepted surfaces within a small footprint. We chose the average crown width of an old cottonwood tree for a synthetic waveform footprint as a starting point. The modeled large-footprint lidar waveform is sum of the reflections from different parts in the footprint that vertically stacked the elevations produced by the small-footprint elevation data. Fig. 2a contains the three-dimensional distribution of small-footprint lidar data from within a 26 m footprint centered on a tree approximately 30 m tall. Fig. 2b illustrates the distribution of these points as a function of height. As in Blair and Hofton's (1999) study, we tested the similarity between each modeled waveform and the return waveform from the ILRIS scanner using Pearson correlation, ρ, given by $\rho = S_{xy} / \sqrt{S_{xx}S_{yy}}$, where Sxx , Syy and Sxy are the variances and shared variance of the ILRIS and synthetic waveforms. The waveform comparison utilized 2004 airborne lidar and 2004 ground-based ILRIS data.

Figure 3 plots five synthetic waveforms and corresponding ILRIS return waveforms. The results of comparison of the modeled waveform and the return waveform from ILRIS for old cottonwood trees are presented in Fig. 3a-c. In this case, the highest ρ was 0.73 between the modeled and ILRIS waveforms. Fig. 3d-e contains the waveforms comparing modeled and ILRIS for mature cottonwoods. The highest ρ value increased from 0.73 to 0.75 when mature cottonwoods were considered. Simple, single modal waveforms are typically returned from flat, unvegetated ground surfaces (Figs. 3a and 3e). The modeled and ILRIS waveforms from vegetated regions were multi-modal, each mode representing a vertically-distinct, consolidated layer within the canopy.

Overall, the ground and airborne-based waveforms had a good degree of correlation. Although the modeled and ILRIS waveforms identify reflecting layers at the same elevations, the relative strengths of reflections from those layers varied. The systematic difference noted between modeled and ILRIS waveforms was the consistently-higher amplitude of the canopy response in the ILRIS return waveform (e.g. Fig. 3a). This difference is due to the first-return only nature of the ILRIS system, and a different view angle configuration between the airborne and ILRIS sensors. Also, a large gap through the canopy along the beam path may result in reduction of the amplitude of the canopy response in the modeled return waveform using the airborne system. Furthermore, the ILRIS system presents difficulties in detecting the uppermost portion of old cottonwood tree canopies because of the conical and flat-topped nature of the tree crown. However, the top portion of the crown may not be of sufficient area to register as a significant reflecting surface and therefore may not be detected well.

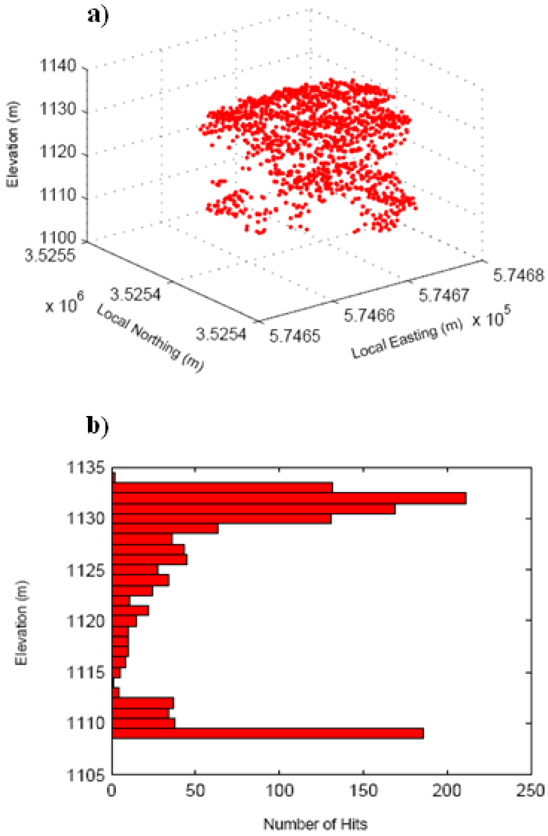

Figure 2. Illustration of the potential for creating synthetic lidar waveforms from small-footprint lidar data.

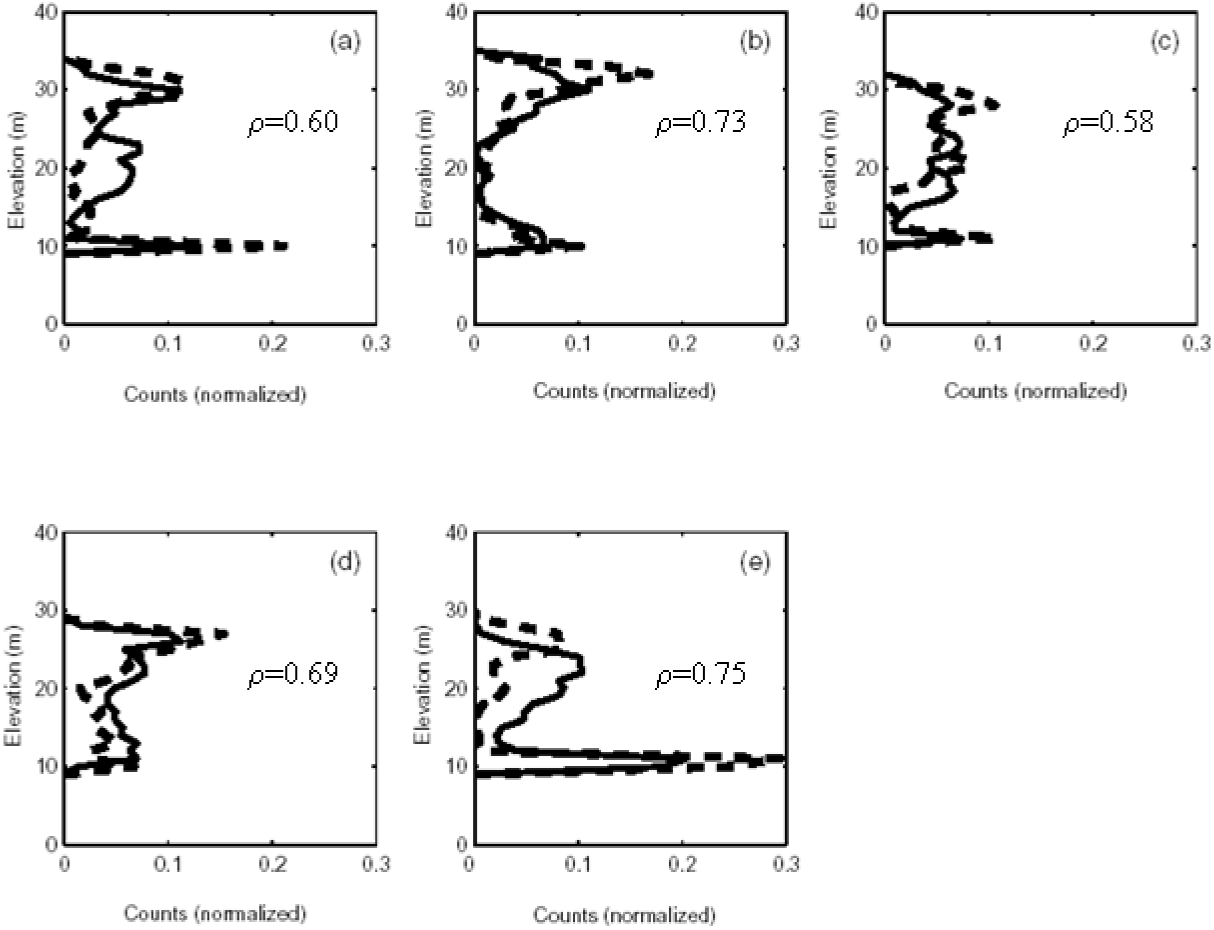

Figure 3. ILRIS (solid line) and modeled (dashed line) waveforms for (a-c) old and (d-e) mature cottonwood trees. ρ is the Pearson correlation coefficient.

Estimation of LAI from Synthetic Lidar Full-waveforms

Four metrics were derived by synthetically constructing a large footprint lidar waveform (see Fig. 4) from the airborne small-footprint lidar data for different age classes of cottonwoods. Lidar canopy height (LHT) was calculated by identifying: (1) the location within the waveform when the first Gaussian pulse increased above a median energy level/threshold (the canopy top), and (2) the center of the last Gaussian pulse (the ground return), and then calculating the distance between these locations. Second, the height of median energy (HOME) was calculated by finding the median of the entire waveform. The location of the median energy was then referenced to the center of the last Gaussian pulse to derive a height. The HOME metric is, therefore, predicted to be sensitive to changes in both the vertical arrangement of canopy elements and the degree of canopy openness (Drake et al., 2002). Third, a simple ground return ratio (GRND) was calculated by taking the number of hits in the last Gaussian peak divided by the sum of all other numbers of hits (total hits minus last Gaussian peak hits) (see Fig. 4). Thus, GRND provides an approximation of the degree of canopy closure (Drake et al., 2002; Means et al., 1999). Finally, the canopy return ratio (CRND) was calculated by taking the number of hits in the location within the waveform when the first Gaussian pulse increases above a median energy level/threshold (the canopy top), divided by the sum of all other numbers of hits. CRND provides an approximation of the degree of canopy cover.

These four metrics were incorporated into a stepwise regression procedure to predict field-derived LAI for different age classes of cottonwoods. During this process, transformations of dependent and independent variables (including square, square root, and logarithmic) were also explored (Table 1). Metrics from the lidar waveform are able to estimate LAI for different age classes of cottonwood trees, though in all cases logarithmic transformation of the dependent variable was necessary. In this case, the coefficient of determination for field LAI versus lidar metrics were 0.76, 0.78, and 0.84 for young, mature, and old, respectively. Meanwhile, the RMSE for all age classes is low.

The weaker relationship between field LAI and lidar metrics in young trees could be affected by two factors. First, the level of variability in old tree structure at the scale of a waveform is higher than for a young one. A second contributing factor is the presence of gaps in young canopies, which allowed a number of the laser pulses to penetrate the canopy, generating lower values for CRND.

Also, in areas with densely packed canopy materials such as old canopies, fewer lidar pulses will reach the ground, thereby increasing HOME. Conversely, in more open or disturbed areas (e.g., a young tree canopy), more lidar pulses will reach the ground, reducing HOME. Additionally, the height metrics (e.g., LHT and HOME) are the most sensitive, and increase with increasing cottonwood tree age and basal area. The LHT is perhaps the metric with the strongest potential for estimating riparian forest structural characteristics. The LHT metric is influenced by the highest detectable canopy surface within a footprint.

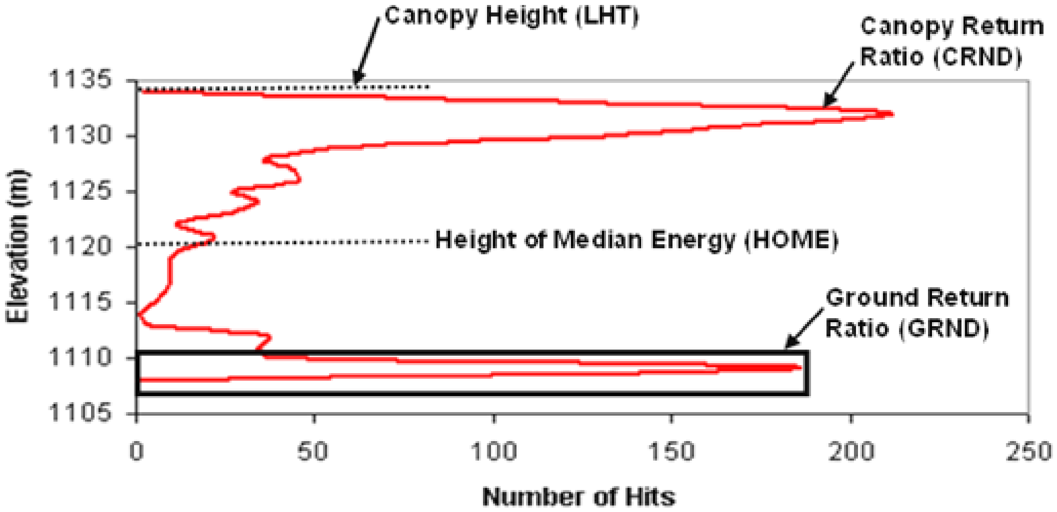

Figure 4. Metrics derived from synthetic large footprint lidar waveforms. These metrics were then used to estimate LAI for different age classes of cottonwoods.

Estimation of Cottonwood Transpiration from Lidar Data

we present the lidar-predicted versus sap flow measured cottonwood transpirations at two contrasting riparian sites in order to more accurately estimate cottonwood water use. Along the San Pedro River, Gazal et al. (2006) quantified cottonwood transpiration using sap flow measurements for an isolated cluster of trees located on a perennial section of the river and another located along a reach with intermittent stream flow. Hydrologically, these sites differed in the depth and seasonal fluctuation of the water table.

The Penman-Monteith (P-M) model (Monteith and Unsworth, 1990) was selected to estimate cottonwood transpiration using lidar-derived LAI for June 1 through June 11, 2003 (DOY: 152-162). This model allows the calculation of evaporation from meteorological variables and resistances which are related to the stomatal and aerodynamic characteristics of the tree.

The aerodynamic resistance (r_a) is the sum of the turbulent resistance between the canopy and the atmosphere from turbulent eddies and the boundary layer resistance (Thom, 1975). Due to the relatively open nature of the cottonwood canopy, the turbulent canopy resistance is assumed negligible in comparison to the boundary layer resistance (Goodrich et al., 2000). Hence r_a is assumed to equal the boundary layer resistance (r_b). To estimate the boundary layer resistance, the model proposed by Choudhury and Monteith (1988) was used:

$$r_b = \frac{1}{(LAI)(b)} \frac{\alpha_{att}}{(1 - \exp(-\frac{1}{2}\alpha_{att}))} \sqrt{\frac{\omega}{U}}$$

In this equation, LAI is the canopy projected leaf area index (the same as leaf area index) derived from synthetic large footprint lidar. The quantity b was set equal to 0.0067 m $s^{-1/2}$. It is a scaling coefficient for leaf boundary layer resistance (Magnani et al., 1998). α_{att} is an attenuation coefficient for wind speed inside the canopy, $\omega = 0.05$ m is a typical leaf width, and U the wind speed outside the canopy (measured at 10 m above the ground). The value for the wind attenuation coefficient, α_{att}, was set equal to 3 following Magnani et al. (1998). The only remaining quantity required to compute cottonwood transpiration is the bulk canopy resistance (r_c). The canopy resistance is related to individual leaf stomatal resistance (r_s) by the following expression (Goodrich et al., 2000):

$$r_c = \frac{r_s}{2LAI}$$

r_s was estimated by Gazal et al. (2006) at both sites. LAI was derived for both sites using the modeled waveform lidar and from ground-based measurements (LAI 2000, Li-Cor, Inc., Lincoln, NE; Gazal et al., 2006). The lidar-derived LAI at the perennial was 3.48 and at intermittent stream site was 2.78. It was assumed that these values were constant over the study period (DOY: 152-162) centered around the lidar flight.

Daily total lidar-predicted transpiration of the cottonwoods at the perennial stream site was higher than that at the intermittent stream site throughout the study period (Fig. 5). Total lidar-predicted E was 23 mm at the intermittent stream site, and 55 mm at the perennial stream site. This is consistent with Schaeffer et al. (2000) who found that riparian water use was correlated to LAI. Depth to groundwater (d_{gw}) at the intermittent stream site was deeper than at the perennial stream site. At the intermittent stream site, d_{gw} increased from 3.1 m during the early part of the spring season to 3.9 m during the peak of the drought period (Gazal et al., 2006). At the perennial stream site, d_{gw} had a gradual but much smaller decline during the pre-monsoon drought. The depth at the beginning of the spring season was 1.5 m and increased to only 1.8 m at the peak of the drought period (0.5 m less than at the intermittent site; Gazal et al., 2006). Thus, greater depths to groundwater corresponded with lower rates of lidar-predicted LAI and transpiration. Additionally, r_s at the intermittent stream site was greater than at the perennial stream site with maximum r_s attained at the peak of the pre-monsoon drought period (Gazal et al., 2006). At the intermittent stream site, the combination of decreased LAI and the increase in r_s caused large reductions in lidar-predicted transpiration that may be associated with both loss of leaf area and the loss of hydraulic conductivity that also facilitated a reduction in stomatal conductance.

Lidar-predicted transpiration of the cottonwoods at two stream sites was 2-5% more than their sap flow measurements (Fig. 6). The differences in lidar-derived LAI and ground-based measurements of LAI (LAI 2000, Li-Cor, Inc., Lincoln, NE; Gazal et al., 2006) account for most of the differences in the magnitude of E. Lidar-derived LAI was greater than ground-based measured LAI at two stream sites. Hence, greater LAI values corresponded with higher rates of cottonwood transpiration at two contrasting riparian sites.

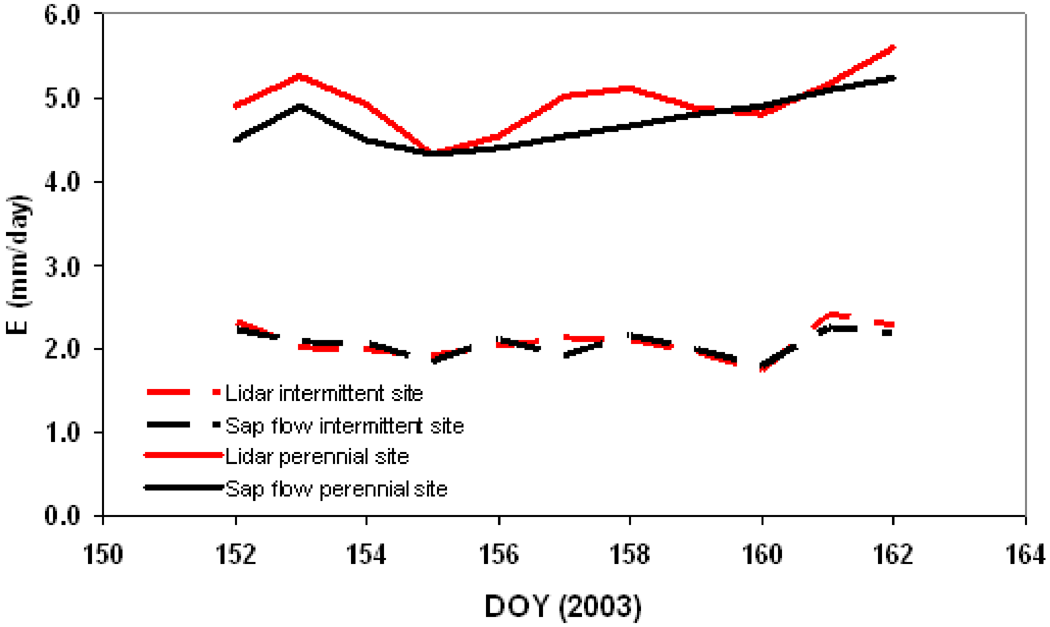

Figure 5. Daily total lidar-predicted versus sap flow measured cottonwood transpirations at the intermittent and perennial stream sites.

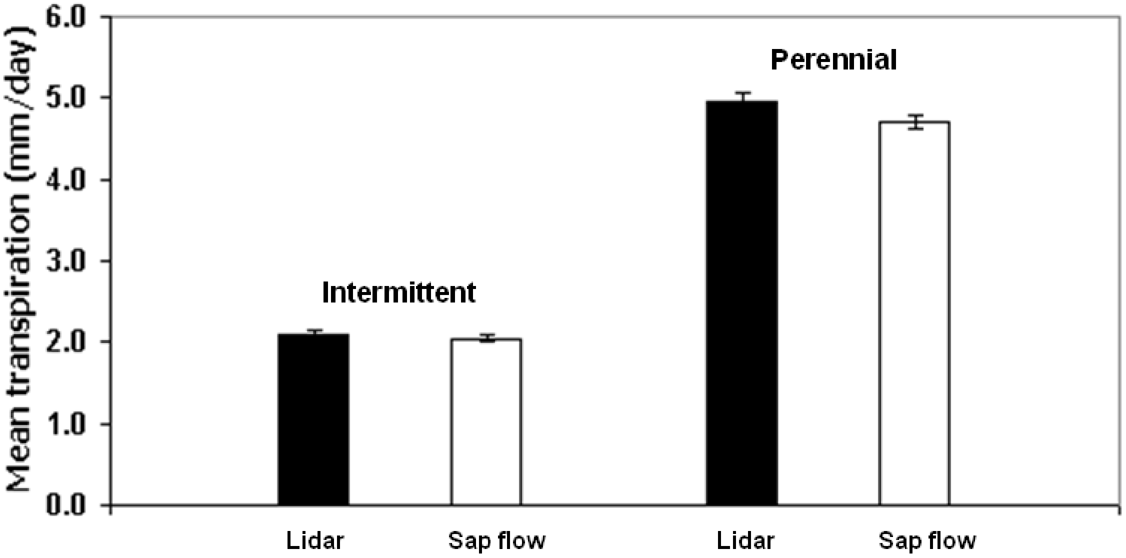

Figure 6. The lidar-predicted versus sap flow measured cottonwood mean daily transpirations at the intermittent and perennial stream sites over an eleven day period centered on the lidar flight.

CONCLUSIONS

We have shown that one can synthesize the vertical structure information for cottonwood trees in a medium-large footprint laser altimeter return waveform using a small-footprint elevation data set. The similarity between modeled waveform and return waveform from ILRIS scanner was assessed using the Pearson correlation statistic. Overall, the waveforms had a good degree of correlation. Although the modeled and ILRIS waveforms identify reflecting layers at the same elevations, the relative strengths of reflections from those layers varied. In addition, cottonwood tree-age changes are likely mirrored in the shape or vertical geolocation of the waveform.

For each cottonwood tree, four metrics were derived from the modeled large-footprint return waveforms for different age classes of cottonwood trees in a riparian corridor. These four metrics were incorporated into a stepwise regression procedure to predict field-derived LAI. The metrics from the lidar waveform were able to estimate LAI for different age classes of cottonwood trees, though in all cases logarithmic transformation of the dependent variable was necessary.

Lidar and meteorological based estimates of cottonwood transpiration versus sap flow estimated transpiration at perennial and intermittent riparian sites were also made. Lidar-met-based transpiration estimates of the cottonwood at the two stream sites were 2-5% greater than their sap flow measurements over an eleven day period centered on the lidar flight. The differences in lidar-derived LAI and ground-based measurements of LAI account for most of the differences in the magnitude of E.

Overall, airborne lidar offers the distinct advantage of providing LAI estimates over large areas which can than be used to improved riparian water-use estimates. Airborne, multi-return small-footprint lidar systems are becoming more widely available and the cost of lidar data acquisition is expected to continue to decrease. This study primarily concentrated on individual cottonwood trees to develop the relationships to estimate LAI for riparian water use estimates and may not be applicable to dense, overlapping canopies. Additionally, lidar cannot provide information on stomatal control with also regulates riparian cottonwood water use so independent estimates or typical ranges of canopy level stomatal resistance will be required. However, strategically acquired lidar data and derived spatially explicit LAI measurements, offer significant potential to improve corridor level riparian water use estimates.

REFERENCES

Abshire, J.B., J.F. McGarry, L.K. Pacini, J.B. Blair, and G.C. Elman, 1994. Laser Altimetry Simulator Version 3.0 User's Guide, NASA Technical Memorandum 104588, Greenbelt, Maryland, 70.

Blair, J.B., and M.A. Hofton, 1999. Modeling laser altimeter return waveforms over complex vegetation using high-resolution elevation data, *Geophysical Research Letters*, 26, 2509-2512.

Choudhury, B.J., and J.L. Monteith, 1988. A four-layer model for the heat budget of homogeneous land surfaces, *Quarterly Journal of Royal Meteorological Society*, 114, 373-398.

Drake, J.B., R.O. Dubayah, D.B. Clark, R.G. Knox, J.B. Blair, M.A. Hofton, R.L. Chazdon, J.F. Weishampel, and S.D. Prince, 2002. Estimation of tropical forest structural characteristics using large-footprint lidar, *Remote Sensing of Environment*, 79, 305-319.

Farid, A., D. Rautenkranz, D.C. Goodrich, S.E. Marsh, and S. Sorooshian, 2006a. Riparian vegetation classification from airborne laser scanning data with an emphasis on cottonwood trees, *Canadian Journal of Remote Sensing*, 32, 15-18.

Farid, A., D.C. Goodrich, and S. Sorooshian, 2006b. Using airborne lidar to discern age classes of cottonwood trees in a riparian area, *Western Journal of Applied Forestry*, 21, 149-158.

Gardner, C.S., 1992. Ranging performance of satellite laser altimeters, I*EEE Transactions on Geoscience and Remote Sensing,* 30, 1061-1072.

Gazal, R.M., R.S. Scott, D.C. Goodrich, and D.G. Williams, 2006. Controls on transpiration in a semiarid riparian cottonwood forest, *Agricultural and Forest Meteorology*, 137, 56-67.

Goodrich, D.C., R. Scott, J. Qi, B. Goff, C.L. Unkrich, M.S. Moran, D. Williams, S. Schaeffer, K. Snyder, R. Macnish, T. Maddock, D. Pool, A. Chehbouni, D.I. Cooper, W.E. Eichinger, W.J. Shuttleworth, Y. Kerr, R. Marsett, and W. Ni, 2000. Seasonal estimates of riparian evapotranspiration using remote and in-situ measurements, *Agricultural and Forest Meteorology*, 105, 281-309.

Maclean, G.A., and W.B. Krabill, 1986. Gross-merchantable timber volume estimation using an airborne LIDAR system, *Canadian Journal of Remote Sensing*, 12, 7-18.

Magnani, F., S. Leonardi, R. Tognetti, J. Grace, and M. Borghetti, 1998. Modelling the surface conductance of a broadleaf canopy: effects of partial decoupling from the atmosphere, Plant, *Cell Environment*, 21, 867-879.

Means, J.E., S.A. Acker, D.J. Harding, J.B. Blair, M.A. Lefsky, W.B. Cohen, M. Harmon, and W.A. McKee, 1999. Use of large-footprint scanning airborne lidar to estimate forest stand characteristics in the western Cascades of Oregon, *Remote Sensing of Environment*, 67, 298-308.

Means, J.E., 2000. Comparison of large-footprint and small-footprint lidar systems: Design, capabilities, and uses, in *Proceedings of Second International Conference on Geospatial Information in Agriculture and Forestry*, Lake Buena Vista, Florida, 85-192.

Monteith, J.L., and M.H.Unsworth, 1990. *Principles of Environmental Physics*, Edward Arnold, London, England.

Nelson, R.F., W.B. Krabill, and G.A. Maclean, 1984. Determining forest canopy characteristics using airborne laser data, *Remote Sensing of Environment*, 15, 201-212.

Nelson, R.F., R. Swift, and W.B. Krabill, 1988a. Using airborne lasers to estimate forest canopy and stand characteristics, *Journal of Forestry*, 86, 31-38.

Nelson, R.F., W.B. Krabill, and J. Tonelli, 1988b. Estimating forest biomass and volume using airborne laser data, *Remote Sensing of Environment*, 24, 247-267.

Schaeffer, S.M., D.G. Williams, and D.C. Goodrich, 2000. Transpiration of cottonwood/willow forest estimated from sap flux, *Agricultural and Forest Meteorology*, 105, 257-270.

Scott, R.L., W.J. Shuttleworth, D.C. Goodrich, and T. Maddock III, 2000. The water use of two dominant vegetation communities in a semiarid riparian ecosystem, *Agricultural and Forest Meteorology*, 105, 241-256.

Shuttleworth, W.J., 1993. Evaporation, in: Maidment, D.R. (editor), *Handbook of Hydrology*, McGraw-Hill, New York, 4.1-4.53.

Stromberg, J.C., 1998. Dynamics of Fremont cottonwood (Populus fremontii) and saltcedar (Tamarix chinensis) populations along the San Pedro River, Arizona, *Journal of Arid Environments*, 40, 133-155.

Thom, A.S., 1975. Momentum, mass and heat exchange of plant communities, in: Monteith, J.L. (editor), *Vegetation and the Atmosphere*, Academic Press, New York, 57-109.

U.S. Department of the Interior, 2006. Water management of the regional aquifer in the Sierra Vista sub watershed, Arizona - Report to Congress: U.S. Geological Survey, 26.

Wehr, A., and U. Lohr, 1999. Airborne laser scanning-an introduction and overview, *ISPRS Journal of Photogrammetry and Remote Sensing*, 54, 68-82.

World Rivers Review, 1997. Biodiversity, North America, *World Rivers Review*, News Briefs 12, February 1997. International Rivers Network, Internet document: http://www.irn.org/pubs/wrr/9701/briefs.html (last date accessed: 15 May 2004).